Published in final edited form as:
Mol Pharm. 2011 February 7; 8(1): 143–152. doi:10.1021/mp100203a.

Modulation of CD4+ T Lymphocyte Lineage Outcomes with Targeted, Nanoparticle-Mediated Cytokine Delivery

Jason Park[1,&], **Wenda Gao**[2,&], **Roy Whiston**[3], **Terry B. Strom**[2], **Su Metcalfe**[3], and **Tarek M. Fahmy**[1]

[1] Yale University, Department of Biomedical Engineering, 55 Prospect Street, 415 Malone Engineering Center, New Haven, CT 06511

[2] Harvard University and Beth Israel Deaconess Medical Center, The Transplant Institute, 330 Brookline Avenue, SL-429, Boston, MA 02215

[3] University of Cambridge**, Department of Surgery, Box 202, Level E9, Addenbrooke's Hospital, Hills Road, Cambridge CB2 2QQ United Kingdom

Abstract

Within the immune system there is an exquisite ability to discriminate between "self " and "non-self" that is orchestrated by antigen-specific T lymphocytes. Genomic plasticity enables differentiation of naïve CD4+ T lymphocytes into either regulatory cells (Treg) that express the transcription factor Foxp3 and actively prevent auto-immune self destruction, or effector cells (Teff) that attack and destroy their cognate target. An example of such plasticity is our recent discovery that leukemia inhibitory factor (LIF) supports Treg maturation in contrast to IL-6 which drives development of the pathogenic Th17 effector phenotype. This has revealed a LIF/IL6 axis in T cell development which can be exploited for modulation using targeted cytokine delivery. Here we demonstrate that LIF-loaded nanoparticles (NPs) directed to CD4+ T cells (i) oppose IL6-driven Th17 development; (ii) prolong survival of vascularized heart grafts in mice; and (iii) expand FOXP3+ CD4+ T cell numbers in a non-human primate model *in vitro*. In contrast, IL-6 loaded nanoparticles directed to CD4+ T cells increase Th17 development. Notably, nanoparticle-mediated delivery was demonstrated to be critical: unloaded nanoparticles and soluble LIF or IL-6 controls failed to recapitulate the efficacy of cytokine-loaded nanoparticles in induction and/or expansion of Foxp3+ cells or Th17 cells. Thus, this targeted nanoparticle approach is able to harness endogenous immune-regulatory pathways, providing a powerful new method to modulating T cell developmental plasticity in immune-mediated disease indications.

Correspondence to: Su Metcalfe; Tarek M. Fahmy.

&These authors contributed equally to this work

**Currently Brain Repair Centre, University of Cambridge, CB1 2PY, UK

Competing Interests Statement

The authors declare no competing financial interests.

Author Contributions

J.P. W.G. S.M. and T.M.F designed all experiments for this study. J.P developed and characterized nanoparticle formulations. J.P and W.G. performed *in vitro* cell stimulation experiments and were responsible for FACS analyses. W.G. performed allogeneic cell transplant experiments. RW performed the rhesus monkey MLR experiments. J.P. and S.M. wrote the manuscript and J.P., S.M. and T.M.F. edited the manuscript with contributions from all authors.

Supporting Information Available

This information is available free of charge via the Internet at http://pubs.acs.org/.

Keywords

Nanoparticle; leukemia inhibitory factor (LIF); regulatory T cell (Treg); cytokine; targeted delivery; immunotherapy

Introduction

In immune competent individuals, antigen-specific CD4+ T lymphocytes play a critical role in immune discrimination between "self" and "non-self", permitting self-tolerance to co-exist with immunity against foreign pathogens. Within the family of CD4+ T cells, a subset of CD4+Foxp3+ T cells known as "regulatory" T cells (Treg) maintain peripheral self-tolerance; Foxp3 is the critical transcription factor required for Treg lineage development. It is now recognized that Tregs provide a potential resource for antigen-specific tolerogenic therapy for treatment of autoimmune diseases as well as acceptance of organ or tissue allografts, including bone marrow and stem cell grafts in regenerative medicine [1,2].

In the periphery, naïve CD4+ T lymphocytes are quiescent until cognate antigen is recognized, resulting in activation through the antigen-specific T-cell receptor (TCR). The outcome of this activation is regulated by the microenvironment, which includes the strength of signaling through the TCR, concurrent co-stimulatory or inhibitory signals, and the composition of the cytokine milieu. The cytokine milieu specifically is critical for orchestration of lineage development towards aggressive effector T cell (Teff) or tolerant Treg phenotypes [3]. Interleukin-6 (IL-6) is a potent inflammatory cytokine and IL-6 target genes in T cells include RORγt, the Th17 lineage-specific transcription factor. Inappropriate Th17 cell activity may cause pathogenic inflammatory disease, including rheumatoid arthritis and inflammatory bowel disease [4]. IL-6 belongs to the IL-6 family of structurally-related cytokines where activity is qualified by their receptors, these having a common gp130 subunit combined with specific subunits that define cytokine reactivity [5]. Leukemia inhibitory factor (LIF) is also a member of the IL-6 family, with a similar crystal structure (Fig. 1A) but, in marked contrast to IL-6, LIF is associated with Tregs and immune tolerance [6]. Given the profound consequences of the effects of IL-6-related cytokines on T cell lineage differentiation, mechanistic studies sought to identify any direct relationship between LIF and IL-6 signaling in T cells. A counter-regulatory LIF/IL-6 axis was discovered, where this LIF/IL-6 axis is directly linked to the Treg (Foxp3 and LIF) and Th17 (RORγt and IL-6) T cell lineage specification [7]. The therapeutic implications of the LIF/IL6 axis may thus, enable antigen-specific guidance of immune tolerance in vivo via LIF.

Cytokine-based therapeutics are generally limited by short cytokine half-lives and serum protease-mediated degradation[8], these being natural mechanisms that normally attenuate the powerful effects of cytokines. However, the therapeutic effect of IL-2 has been greatly improved by prolonging its half-life by the attachment of fusion molecules such as polyethylene glycol (PEG)[9] or humanized antibody fragments [10]. We therefore considered that it may be possible to manipulate LIF for therapy and here our choice was to use biodegradable nanoparticles (NPs) since NPs offer multiple advantages as drug delivery vehicles for cytokine-related therapies, including protection from rapid degradation; prolonged delivery through sustained release; and targeting to specific cell types [11]. The polymer poly(lactide-co-glycolide) (PLGA) is already approved by the FDA for drug delivery applications due to its safety, excellent biocompatibility, and "tunable" release rates. In NP form, PLGA decorated with functional avidin groups on the nanoparticle surface enables modification of the surface through the robust attachment of biotinylated ligands such as PEG [12], T cell-stimulating antibodies [13], and T cell-targeting antibodies

[14] (Fig. 1B). This technology is well-suited towards stimulation and manipulation of immune cell development through (i) the presence of T cell-specific cell surface molecules that can be targeted by antibody; (ii) on the NP, presentation of multiple targeting ligands per nanoparticle ensuring high valency and avidity of contact with targeted cellular ligands; and (iii) delivery of multiple cytokine molecules per biorecognition event to ensure relatively high concentration of cytokine precisely within the microenvironment of the targeted cell, whilst avoiding systemic exposure to the therapeutic cytokine.

In this investigation we have not only confirmed that the LIF/IL6 axis can be recapitulated in T cells treated with LIF-NP/IL6-NP, but also that the nanoparticulate therapeutic approach is underpinned by controlled, sustained release of bioactive LIF or IL-6 in low, physiological doses within the precise microenvironment of the target cell.

Experimental Section

Nanoparticle formulation and characterization

Human LIF (Santa Cruz cat. SC-4377), mouse LIF (Santa Cruz cat. SC-4378), or recombinant mouse IL-6 (eBioscience cat. 14-8061-80) was encapsulated in avidin-coated PLGA nanoparticles using a modified water/oil/water double emulsion technique. Briefly, 50 μg of cytokine was dissolved in 200 μL PBS and added dropwise with vortexing to 100 mg PGLA (50/50 monomer ratio, Durect Corp. cat. B0610-2) in 2 ml dichloromethane. The resulting emulsion was added to 4 ml of aqueous surfactant solution containing 2.5 mg/ml polyvinyl alcohol (PVA) (Sigma-Aldrich cat. 363138) and 2.5 mg/ml avidin-palmitate bioconjugate (previously described [15]), and sonicated to create an emulsion containing nano-sized droplets of polymer/solvent, encapsulated cytokine and surfactant. Solvent was removed by magnetic stirring at room temperature; hardened nanoparticles were then washed 3x in DI water and lyophilized for long-term storage. CD4-targeted nanoparticles were formed by reacting avidin-coated NPs in PBS with 4 μl biotin-anti-CD4 (0.5 mg/ml) per mg NP for 15 minutes and used immediately. Nanoparticle size and morphology were analyzed via scanning electron microscopy and dynamic light scattering in 1x PBS (Brookhaven Instruments, ZetaPALS). Cytokine release was measured by incubating particles in PBS at 37°C and measuring cytokine concentrations in supernatant fractions by ELISA. Total encapsulation was approximated as the amount of LIF or IL-6 released over a seven day period and percent encapsulation efficiency calculated as total encapsulation divided by maximum theoretical encapsulation. Capture of biotinylated ligands was quantified using biotin-R-phycoerythrin as a model protein. NPs were suspended at 1.0 mg/ml in 1x PBS, and 200 ul added to eppendorfs containing varying concentrations of biotin-R-PE. NPs were reacted for 15–30 minutes at room temperature, centrifuged for 10 minutes at 12k RPM, and the remaining biotin-R-PE in the supernatant quantified by fluorescence at excitation/emission 533/575nm. All data are presented as mean ± standard deviation.

Animals

Foxp3-GFP knockin mice were generated on a C57BL/6 background as previously described [16], then backcrossed for 8 generations onto the BALB/C background. DBA/2 mice were purchased from Jackson Laboratory. BALB/c and CBA mice were purchased from Harlan for use at 10 – 12 weeks of age.

In vitro T cell stimulation

As previously described [7] FACS-sorted CD4+GFP- mouse naive cells were stimulated in flat bottomed 96-well plates with plate-bound anti-CD3 (10 μg/ml), soluble anti-CD28 (1 μg/ml), and IL-2 (50 ng/ml). For Foxp3+ Treg induction, cultures were supplemented with TGF-β (5 ng/ml). For Th17 induction, cultures were supplemented with TGF-β and IL-6 (20

ng/ml). All concentrations account for total well volume after addition of control media or nanoparticle-containing media.

Cells were imaged by SEM and fluorescent microscopy after incubation with or without CD4-targeted NPs. For SEM, naïve CD4+ T cells were stimulated for 24 hours with or without CD4-targeted LIF-nano. Cells were collected by centrifugation (3000 RPM), fixed in 4% paraformaldehyde + 0.1% glutaraldehyde for 15′ and then in 4% paraformaldehyde for an additional 45′ before being washed twice in 1x PBS. For fluorescent experiments, naïve CD4+ T cells were incubated with or without CD4-targeted nanoparticles containing coumarin-6 for 2 hours at either 37° or 4°C. Cells were fixed in 4% paraformaldehyde for 1 hour, permeabilized with 0.1% Triton-X100, and washed in PBS. Cell nuclei and cytoskeleton were stained using DAPI and Texas-Red phalloidin.

For the non-human primate (NHP) MLR experiments, blood samples from mismatched Rhesus monkeys were obtained from the Biomedical Primate Research Centre, Rijswijk, Netherlands. Using peripheral blood mononuclear cells, the MLR general procedure followed that described by Haandstra et al. [17]. The current experiments employed one way MLR cultures co-mixed in bulk then aliquoted in triplicate into round-bottomed microtitre wells containing either (i) LIF-nanoparticles targeted to CD4 (biotin-anti-human CD4 from eBioscience cat. 13-0049); (ii) empty-nanoparticles targeted to CD4; (iii) soluble recombinant human LIF (10ng/ml); (iv) soluble recombinant human IL6 (10ng/ml); (v) soluble LIF plus anti-hIL6 (R&D AB-206-NA); (vi) soluble IL6 plus anti-hLIF; (vii) no additions (control). All treatment stocks were freshly prepared. Replicate plates were analyzed by flow cytometry for CD4, CD25 and FOXP3 (eBioscience human/NHP Treg staining kit) at 7d and at 11d: for the 11 day cultures, the cultures were re-boosted at 7d with fresh irradiated donor pbmc. In addition to percent distribution counts, actual numbers of FOXP3 positive cells per well were calculated.

In vivo donor-specific transfusion (DST)

As previously described [7] DBA/2 splenocytes were treated for 15 minutes with CD4-targeted unloaded (empty), LIF-loaded, or IL-6-loaded nanoparticles. The NP-bound cells (10^7 per mouse) were infused i/v into BALB/c Foxp3-GFP mice (n=3 per group). Lymph nodes were harvested after 5 days and the ratio of GFP+ (Treg) to GFP- CD4+ cells were calculated in donor-specific Vβ6 or non-specific Vβ8. Data are reported as mean ± standard deviation.

Mismatched murine heart allograft transplant rejection

Vascularised mouse heart allografts from BALB/c donors to the neck of CBA recipients followed previously published procedures [18]. BALB/c to CBA is a full mismatch combination that results in graft rejection at ~7d in untreated controls, as determined by cessation of grafted heart beat. At 0d, experimental groups received either (i) nothing; (ii) CD4-targeted empty nanoparticles; (iii) a donor-specific blood transfusion (DST) i.p. of 2×10^7 BALB/c spleen cells; or (iv) DST premixed with CD4-targeted LIF-nanoparticles. All treatments were i.p. and as a single dose on day of transplant.

Results

CD4-targeted PLGA nanoparticles deliver bioactive LIF and IL-6

Avidin-coated PLGA nanoparticles were observed by scanning electron microscopy to be discrete and spherical (Fig. 2A). Nanoparticle diameters were calculated to be 100 ± 20 nm (mean ± S.D.) by Scion Image software (Fig. 2B). Nanoparticle hydrodynamic diameter was analyzed by dynamic light scattering in 1x PBS. The effect of ligand coating was assessed

by adding 0.1x or 10x molar excess of biotinylated anti-CD4 in serial fashion to LIF-nano. Biotinylated ligands were attached to the nanoparticles immediately prior to use as described in the experimental section and in previous publications [12,13]. Addition of biotinylated anti-CD4 was not found to have a significant effect on the mean effective diameter of nanoparticles in PBS (Fig. 2C). Data are reported as mean ± S.D. of 10 readings with polydispersity index reported in parentheses above columns. Ligand attachment was quantified using biotin-R-PE as a model protein. LIF-nano were incubated with biotin-R-PE in increasing molar concentrations. Surface-coated nanoparticles were then removed by centrifugation and the remaining fraction of biotin-R-PE in the supernatant measured by fluorescence. LIF-nano were found to stably bind up to 6.2 ± 2.3 μg ($1.6 \pm 0.6 \times 10^{13}$ molecules) of biotin-R-PE (mean ± S.D. of all data points) (Fig. 2D). The number of NPs was measured to be between 5×10^{10} to 1×10^{11} NPs per mg by a Nanosight particle tracking instrument. The approximate number of ligands per nanoparticle was therefore calculated by dividing the molecules of biotin-R-PE attached by the number of nanoparticles, leading to an estimate of 100–400 ligands per nanoparticle. Release of IL-6 or LIF from nanoparticles was assessed by incubating samples in triplicate in PBS at 37ºC and measuring cytokine release into the supernatant by ELISA. The cumulative release was measured to be 1000 ± 50 picograms LIF per milligram LIF-nano (Fig. 2E) and 2400 ± 360 picograms IL-6 per milligram IL-6-nano over a 7 day period (Fig. 2F). Release beyond 7 days was not significant. The data represent mean ± S.D. for 3 or more separate samples.

The LIF/IL-6 axis can be modulated *in vitro* using nanotherapy

Activation of naïve CD4+ T cells in the presence of transforming growth factor beta (TGF-β) alone is known to induce Foxp3 expression while, in contrast, activation in the presence of both IL-6 and TGF-β results in ROR T expression [16]. We therefore examined the bioactivity of nanoparticle-delivered LIF or IL-6 and their effect on differentiation of naïve CD4+ T cells *in vitro* through the expression of these lineage-specific transcription factors.

LIF was found to augment the expression of Foxp3. Naïve CD4+ T cells were activated with anti-CD3, anti-CD28, and IL-2 in the presence of 1 ng/ml TGF-β and increasing doses of LIF or LIF-nano. Higher doses of LIF supported development of Foxp3 expression, but interestingly a 0.1 mg/ml dose of LIF-nano was as effective as a 10–100 ng/ml dose of soluble LIF (Fig. 3A), suggesting an approximate 1000-fold increase in potency when adjusting for relative dose by the total 7-day release of LIF from Fig. 2E. This phenomenon was also observed in IL-6-mediated suppression of Foxp3 expression. We found that IL-6-nano were more effective at suppression of Foxp3 than equivalent doses of soluble IL-6 at doses between 1 and 100 pg/ml (Fig. 3B). The maximum dose of NPs given was 0.2 mg/ml, due to cytotoxic effects at higher concentrations (Fig. 3C). However, nanoparticle cytotoxicity was not determined to be a factor at the doses used. PLGA NPs incubated with T cells under standard stimulation conditions did not have cytotoxic effects against CD4+ T cells at concentrations below 0.1 mg/ml (Fig. 3C). Representative FACS plots of the comparative effects of IL-6 and LIF on Foxp3 expression are shown in (Fig. 3D).

LIF-nano and IL-6 nano were found to have counteracting effects on RORγT expression. Naïve CD4+ T cells were activated with anti-CD3, anti-CD28, and IL-2 in the presence of 1 ng/ml TGF-β and increasing doses of IL-6 or IL-6-nano. IL-6-nano were found to induce RORγT expression in greater than 70% of the population at significantly lower doses than soluble IL-6 (Fig. 4A). The minimum effective dose of soluble IL-6 used (1 ng/ml) was found to only induce approximately 40% RORγT expression. Conversely, LIF-nano were found to suppress RORγT expression. In these experiments, naïve CD4+ T cells were activated in media containing 1 ng/ml TGF-β, a high dose (20 ng/ml) of soluble IL-6, and increasing doses of LIF-nano or LIF soluble. Assuming full potential release of 1000 pg LIF per mg NP, nanoparticle-delivered cytokine was observed to be approximately 1000-fold

more potent than soluble LIF in suppression of RORγT (Fig. 4B). We note that LIF therapy at higher doses of either soluble or nanoparticle-loaded cytokine did not demonstrate significant toxic or proliferative effects on CD4+ T cells (Fig. 4C). Representative FACS plots of highest cytokine or nanoparticle doses are shown to highlight the counter-regulatory effect of IL-6 and LIF on RORγT expression (Fig. 4D).

The interaction between T cells and nanoparticles was observed using SEM as well as fluorescent microscopy. Under SEM, CD4+ Tcells were found to be approximately 5 microns in diameter with a relatively smooth surface after 24 hours of stimulation (Fig. 5A). When CD4-targeted LIF-nano was added to the stimulation media, distinct nanoparticles could be observed on the lymphocyte surface even after cells were washed (Fig. 5B). Nanoparticles encapsulating the fluorescent dye coumarin 6 (C6-nano) were used to further visualize T-cell-nanoparticle interactions. CD4+ T cells were incubated with C6-nano at 37°C or 4°C for 2 hours, then washed, fixed, and stained with Texas-Red-phalloidin and DAPI. CD4+ T cells were observed to have large nuclei and intact membrane (Fig 5C). After the addition of CD4-targeted C6-nano, nanoparticles were found associated with the cell surface regardless of temperature (Fig. 5D–E). Thus the observed increase in bioactivity may be due to stable and enhanced interaction of targeted nanoparticles with CD4+ T cells. Unlike our previous report demonstrating significant internalization of PLGA particles by phagocytic dendritic cells[19], we did not observe significant nanoparticle fluorescence within the lymphocyte cytosol. The exact mechanism of enhanced bioactivity remains an area of ongoing investigation, but we note that this observation is consistent with our previous report demonstrating increased bioactivity of IL-2 when delivered from PLGA particles [13].

LIF-nano are tolerogenic *in vivo* in the mouse

We had previously demonstrated that that CD4-targeted LIF-nano bias the *in vivo* immune response towards tolerance, as measured by the relative numbers of antigen-specific Foxp3+CD4+ T cells following donor-specific transfusion (DST) [7]. We repeated these experiments using IL-6-nano to treat lymphocytes prior to DST. Pretreatment of naïve donor CD4+ T cells with CD4-targeted LIF-nano resulted in a nearly 4-fold increase in the ratio of antigen-specific (e.g. vβ6+, solid black bars) GFP+Foxp3+/GFP-Foxp3- cells (Fig. 6A). A slight increase in the Treg ratio was observed with the empty-nano control. This effect is likely due to the presence of anti-CD4 antibodies on the particle surface and is consistent with previous reports demonstrating that anti-CD4 blockade supports foxp3 induction [20,21]. Notably, the effect was abrogated completely when donor cells were pre-treated with CD4-targeted IL-6-nano (Fig. 6A), We therefore conclude that the expansion of antigen-specific Foxp3+ cells is indeed due to the bioactivity of LIF-nano. We then examined whether LIF-nano could be utilized for therapeutic effect in support of a functioning allograft *in vivo*. We used a difficult but highly reproducible mouse model of vascularised heart allografts between fully mismatched donor-recipient mice (BALB/c to CBA). Following allograft transplantation, animals received donor-specific transfusions in similar fashion to the study in (Fig. 5A). Animals receiving no supporting treatment or DST alone suffered graft rejection 7 days after implantation (Fig. 6B). Combination therapy (DST in concert with a single dose of CD4-targeted LIF-nano) at the time of grafting significantly increased mean survival time from 7d to 12d (n=3 or more animals, $p < 0.01$ by Pearson's chi-square analysis). Although analysis of tissue-infiltrating lymphocytes was not conducted due to the endpoint nature of the studies, we note that the increased survival in the DST+LIF treatment group appears to correlate with the group in which the greatest expansion of Tregs in healthy recipient mice was observed (Fig. 6A).

LIF-nano are tolerogenic *in vitro* in the Rhesus monkey

The Rhesus monkey mixed lymphocyte reaction (MLR) was used as a preclinical model to test the efficacy of LIF nanotherapy. Primary MLR's were measured at 7 days and persistence of therapeutically induced effects was measured at 11 days after rechallenge with donor antigen on the 7th day. Treatment with CD4-targeted LIF-nano resulted in a 4-fold increase in percentage of CD4+CD25+FOXP3+ T cells in cultures at 11 days, while empty-nano or soluble LIF had little effect (Fig. 7A). Analysis of the total numbers of cells per culture showed expansion of CD4+ T cells in the CD4-targeted LIF-nano treatment group relative to all other groups (Fig. 7B). Within this expanded CD4+ T cell population, there was greater than 10-fold increase in CD4+CD25+FOXP3+ cells relative to untreated control (Fig 7B).

It was important to establish that any measured effects were due to the delivery of LIF, rather than being a consequence of non-specific CD4+ T cell activation due to crosslinking of the CD4 co-receptor by the delivery vehicle itself. This was clearly demonstrated as empty, CD4-targeted nanoparticles failed to induce Foxp3+ cells (Fig 7B). Secondly, it was important to show that nanoparticle-mediated delivery of LIF was required; this was demonstrated since soluble LIF alone failed to recapitulate the induction of Foxp3+ cells, with only 2-fold increase in CD4+ cell numbers and Foxp3+ expression (Fig 7B). These studies demonstrate that, in addition to in the non-human primates also respond to LIF-nano and that here too the LIF-nano induce expansion of CD4+CD25+FOXP3+ T cells in response to donor antigen; importantly these effects were sustained following further antigenic challenge.

Discussion

Overall, our findings strongly support the notion that endogenous control mechanisms that regulate immune tolerance can be exploited using nanotherapeutic devices to both deliver and release regulatory cytokines in a stable, physiological manner. We have focused our study on LIF, following our previous discovery that LIF is a tolerogenic cytokine able to counter-regulate IL-6. We demonstrate that LIF and IL-6, both members of the IL-6 cytokine family, can be stably encapsulated and released in bioactive form using PLGA nanoparticles. The effect of nanoparticle-delivered cytokine was shown to be highly specific; nanoparticle-delivered LIF was found to enhance Foxp3+ and repress RORγT expression, while nanoparticle-delivered IL-6 induced the opposite effects. This specificity of action is consistent with previous understanding regarding the bioactivity [5,16] of the cytokines and further confirms the critical regulatory axis in T cells that is counter-regulated by LIF and IL-6 [7]. We note that these effects are likely due to their respective receptors, where IL-6 is composed of gp130 homodimers, and LIF of gp130/gp190 heterodimers [5]. Since gp190 is the critical determinant in LIF signaling (and thus in the LIF/IL6 axis) it is highly relevant to note that axotrophin, an RINGv E3-ligase linked to regulatory transplantation tolerance [6], plays a role in degradation of gp190 and has profound regulatory effects on T lymphocytes including their release of endogenous LIF [7,22]

Recent progress in the understanding of the plasticity of T cell fate gives broader significance to these findings. T cell fate between Treg versus Teff may be determined by progressive epigenetic programming that follows activation of the naïve T cell, with lineage commitment becoming progressively more stable and less vulnerable to the immediate micro-environment over time [3,23,24]. It therefore follows that sustained delivery of LIF will in turn sustain the LIF-feed-forward loop towards hard-wiring of the Treg epigenetic profile, including the stable expression of Foxp3. Targeting of LIF-encapsulating nanoparticles to CD4+ T cells enables this specific, sustained delivery of LIF in the face of dynamic physiologic factors such as diffusion and clearance. In the mouse DST and heart

allograft studies, an increase in antigen-specific, Foxp3+ Tregs was only observed when lymphocytes were treated with CD4-targeted LIF-nano – highly localized nanoscale sources of cytokine may represent a significant benefit over any dose of soluble therapeutic.

We believe that LIF-nano-driven immune tolerogenesis heralds a novel, antigen specific approach to immune-mediated disease. Moreover, since LIF is also an important factor for supporting stem cells, the use of LIF-nano in regenerative medicine provides two-fold benefit, supporting engrafted stem cells in addition to protecting them from immune-mediated rejection.

Acknowledgments

We are grateful to Mrs. Sandra Shurey at the Northwick Park Institute for Medical Research Surgical Research Unit for performing the mouse heart allografts; and to Dr Kristina Haanstra and Dr Margreet Jonker of the Biomedical Primate Research Centre, Rijswijk, Netherlands for supplying peripheral blood samples from Rhesus monkeys. We are also grateful to Dr Tim Croudace Department of Psychiatry University of Cambridge who advised on and ran statistical analyses of the mouse heart allograft data. We are also most grateful to Mary Brodey of Lifetechnologies Co for cytokine multiplex testing of Rhesus monkey samples. This work was supported in part by the JDRF (WG and TMF); NIAID (TBS); Addenbrookes Hospital Trust Cambridge UK (SMM); and NIHR Cambridge Biomedical Research Centre (SMM) and an NIH Autoimmunity Center of Excellence grant pilot award to TMF.

References

1. Riley JL, June CH, Blazar BR. Human T regulatory cell therapy: take a billion or so and call me in the morning. Immunity. 2009; 30(5):656–65. [PubMed: 19464988]
2. Masteller EL, Tang Q, Bluestone JA. Antigen-specific regulatory T cells--ex vivo expansion and therapeutic potential. Semin Immunol. 2006; 18(2):103–10. [PubMed: 16458533]
3. Zhou L, Chong MM, Littman DR. Plasticity of CD4+ T cell lineage differentiation. Immunity. 2009; 30(5):646–55. [PubMed: 19464987]
4. Littman DR, Rudensky AY. Th17 and regulatory T cells in mediating and restraining inflammation. Cell. 140(6):845–58. [PubMed: 20303875]
5. Heinrich PC, et al. Principles of interleukin (IL)-6-type cytokine signalling and its regulation. Biochem J. 2003; 374(Pt 1):1–20. [PubMed: 12773095]
6. Metcalfe SM, et al. Leukemia inhibitory factor is linked to regulatory transplantation tolerance. Transplantation. 2005; 79(6):726–30. [PubMed: 15785381]
7. Gao W, et al. Treg versus Th17 lymphocyte lineages are cross-regulated by LIF versus IL-6. Cell Cycle. 2009; 8(9):1444–50. [PubMed: 19342884]
8. Donohue JH, Rosenberg SA. The Fate of Interleukin-2 after Invivo Administration. Journal of Immunology. 1983; 130(5):2203–2208.
9. Delgado C, Francis GE, Fisher D. The Uses and Properties of Peg-Linked Proteins. Critical Reviews in Therapeutic Drug Carrier Systems. 1992; 9(3–4):249–304. [PubMed: 1458545]
10. Strom TB, Koulmanda M. Cytokine related therapies for autoimmune disease. Curr Opin Immunol. 2008; 20(6):676–81. [PubMed: 18940257]
11. Panyam J, Labhasetwar V. Biodegradable nanoparticles for drug and gene delivery to cells and tissue. Advanced Drug Delivery Reviews. 2003; 55(3):329–347. [PubMed: 12628320]
12. Park J, et al. PEGylated PLGA nanoparticles for the improved delivery of doxorubicin. Nanomedicine. 2009; 5(4):410–8. [PubMed: 19341815]
13. Steenblock ER, Fahmy TM. A comprehensive platform for ex vivo T-cell expansion based on biodegradable polymeric artificial antigen-presenting cells. Mol Ther. 2008; 16(4):765–72. [PubMed: 18334990]
14. Fahmy TM, et al. Nanosystems for simultaneous imaging and drug delivery to T cells. Aaps J. 2007; 9(2):E171–80. [PubMed: 17614359]
15. Fahmy TM, et al. Surface modification of biodegradable polyesters with fatty acid conjugates for improved drug targeting. Biomaterials. 2005; 26(28):5727–5736. [PubMed: 15878378]

16. Bettelli E, et al. Reciprocal developmental pathways for the generation of pathogenic effector TH17 and regulatory T cells. Nature. 2006; 441(7090):235–8. [PubMed: 16648838]
17. Haanstra KG, et al. Characterization of naturally occurring CD4+CD25+ regulatory T cells in rhesus monkeys. Transplantation. 2008; 85(8):1185–92. [PubMed: 18431240]
18. Chen ZK, et al. Amplification of natural regulatory immune mechanisms for transplantation tolerance. Transplantation. 1996; 62(9):1200–6. [PubMed: 8932256]
19. Demento SL, et al. Inflammasome-activating nanoparticles as modular systems for optimizing vaccine efficacy. Vaccine. 2009; 27(23):3013–21. [PubMed: 19428913]
20. Cobbold SP, et al. Induction of foxP3+ regulatory T cells in the periphery of T cell receptor transgenic mice tolerized to transplants. J Immunol. 2004; 172(10):6003–10. [PubMed: 15128783]
21. Nagahama K, et al. Differential control of allo-antigen-specific regulatory T cells and effector T cells by anti-CD4 and other agents in establishing transplantation tolerance. Int Immunol. 2009; 21(4):379–91. [PubMed: 19228878]
22. Muthukumarana PA, et al. Evidence for functional inter-relationships between FOXP3, leukaemia inhibitory factor, and axotrophin/MARCH-7 in transplantation tolerance. Int Immunopharmacol. 2006; 6(13–14):1993–2001. [PubMed: 17161353]
23. Josefowicz SZ, Rudensky A. Control of regulatory T cell lineage commitment and maintenance. Immunity. 2009; 30(5):616–25. [PubMed: 19464984]
24. Feuerer M, et al. Foxp3+ regulatory T cells: differentiation, specification, subphenotypes. Nat Immunol. 2009; 10(7):689–95. [PubMed: 19536194]

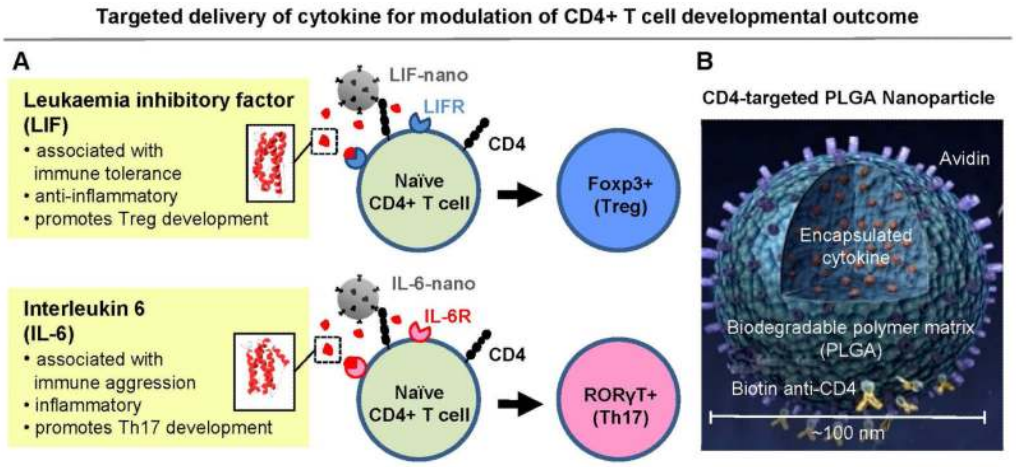

Figure 1. Nanotherapy-mediated modulation of CD4+ T cell differentiation

(A) Schematic model of cytokine-loaded, antibody (anti-CD4)-targeted PLGA nanoparticle. Avidin groups on the nanoparticle surface facilitate attachment of biotinylated targeting antibodies. Hydrolyis of the polymeric matrix releases entrapped, bioactive cytokine in sustained fashion. (B) Prior to *in vitro* stimulation and *in vivo* lymphocyte transfusion experiments (Figs. 2–4), nanoparticles were attached to CD4+ T cells via anti-CD4 antibodies. Nanoparticles encapsulating LIF (LIF-nano) were found to enhance Foxp3 expression, while nanoparticles encapsulating IL-6 (IL-6-nano) enhanced RORγT expression.

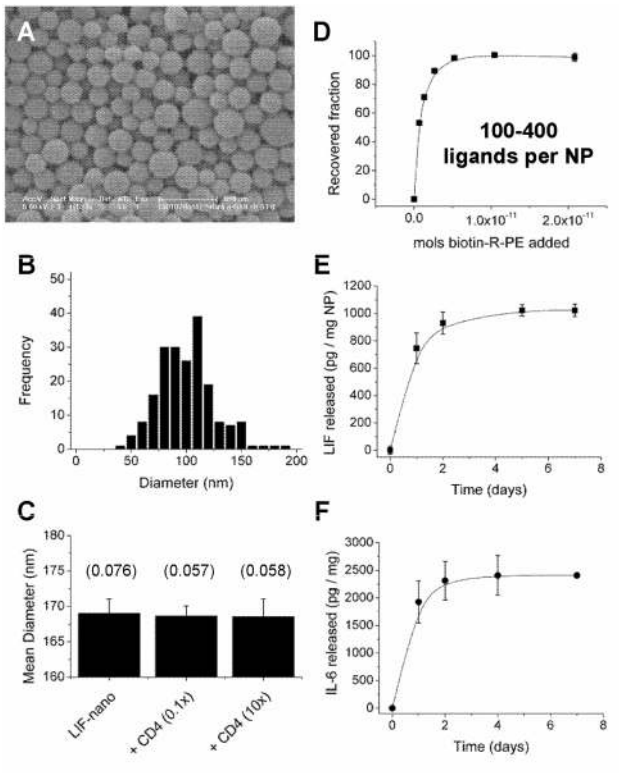

Figure 2. Characterization of cytokine-loaded PLGA nanoparticles

(A) Scanning electron micrograph (SEM) of PLGA nanoparticles. (B) Representative size distribution of PLGA nanoparticles based on analysis of SEM data using Scion image processing software. The mean particle diameter was 100 ± 20 nm (mean ± s.d. of n=3 batches). (C) Effect of ligand attachment on mean effective hydrodynamic diameter, overall sample polydispersity is reported in parentheses above the column. Data represent mean ± S.D. of 10 measurements. (D) Ligand attachment was quantified by measuring NP uptake of biotin-R-PE. LIF-nano were found to bind up to $1.6 \pm 0.6 \times 10^{13}$ molecules of biotin-R-PE per mg NP. Particle counts were between 5×10^{10} and 1×10^{11}NPs/mg. (E) Cumulative release of LIF or (F) IL-6 from PLGA nanoparticles in pg cytokine per milligram nanoparticles. Cytokine concentration was measured by ELISA and data represent mean ± s.d. (n=3 individual samples per time point).

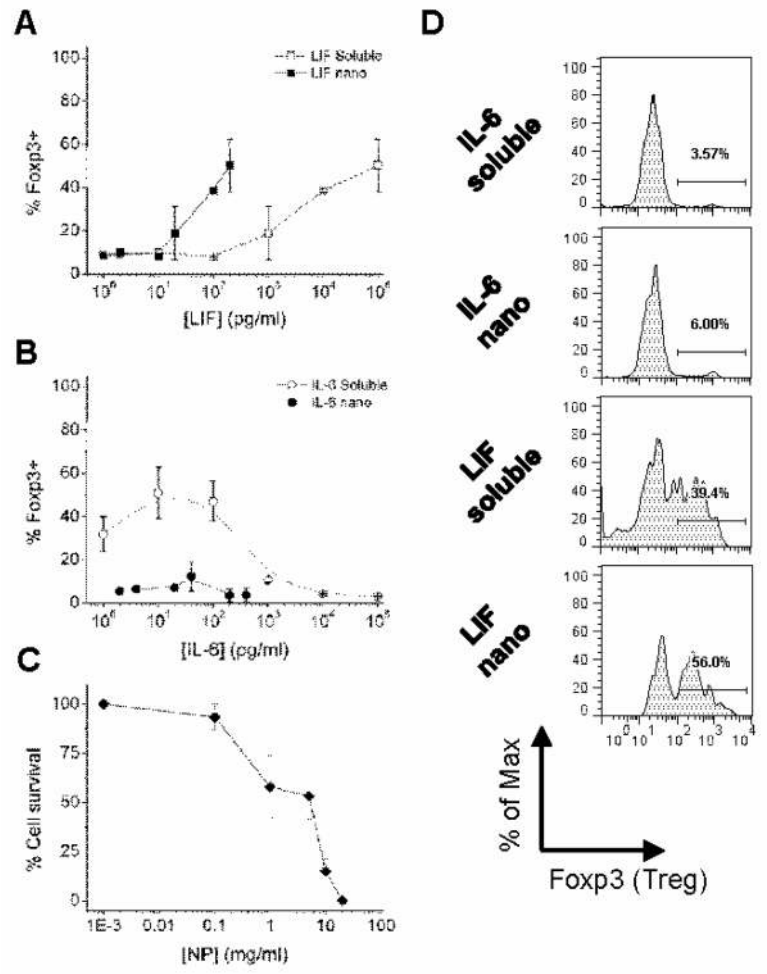

Figure 3. Nanoparticle-delivered LIF and IL-6 have counter-regulatory effects on Foxp3 expression *in vitro*

LIF supports Foxp3 expression following activation in the presence of TGF-β, while IL-6 suppresses Foxp3 expression. (A) Naïve CD4+GFP- T cells were stimulated for 72 hours with plate-bound anti-CD3, soluble anti-CD28, soluble IL-2, soluble TGF-β, and increasing doses of LIF or LIF-nano. Intracellular expression of Foxp3 was assessed via flow cytometry and is shown on the y-axis. Nanoparticle-encapsulated doses of LIF were calculated based on total cumulative release of approximately 1000 pg LIF per mg NP (Fig. 2E). (B) Naïve CD4+GFP- T cells were stimulated in same conditions as in (A) but with increasing doses of IL-6 or IL-6-nano. Nanoparticle doses of IL-6 were estimated to be 2000 pg IL-6 per mg NP from (Fig. 2F). (C) Cytotoxicity of avidin-coated PLGA NPs was assessed by MTT assay. NPs were incubated at increasing concentrations for 72 hours with CD4+ T cells. (D) Representative FACS plots of maximally effective doses from (A) and (B) demonstrate opposing effects of LIF and IL-6 on Foxp3 expression.

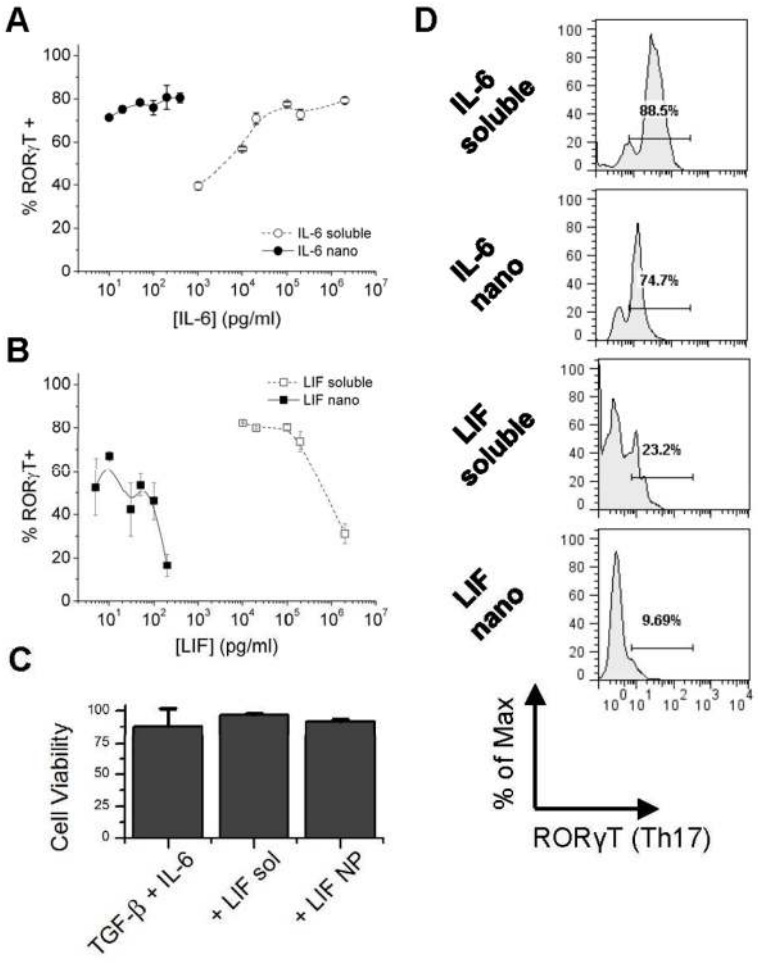

Figure 4. Nanoparticle-delivered LIF and IL-6 have counter-regulatory effects on RORγT expression *in vitro*

IL-6-nano induces RORγT expression following activation in the presence of TGF-β while LIF-nano suppresses IL-6-driven RORγT expression. (A) Naïve CD4+ T cells were stimulated for 72 hours with plate-bound anti-CD3, soluble anti-CD28, soluble IL-2, soluble TGF-β, and increasing doses of IL-6 or IL-6-nano. Expression of RORγT was assessed via flow cytometry and is shown on the y-axis. Nanoparticle dose of IL-6 was estimated to be approximately 2000 pg IL-6 per mg NP from (Fig. 2F). (B) Naïve CD4+ T cells were stimulated in same conditions as in (A) with the addition of 20 ng/ml IL-6 to the media. Nanoparticle dose of LIF was estimated to be 1000 pg LIF per mg NP from (Fig. 2E). (C) Cell viability at maximum shown doses was assessed by MTT assay. (D) Representative FACS plots of maximally effective doses from (A) and (B) demonstrate opposing effects of LIF and IL-6 on RORγT expression.

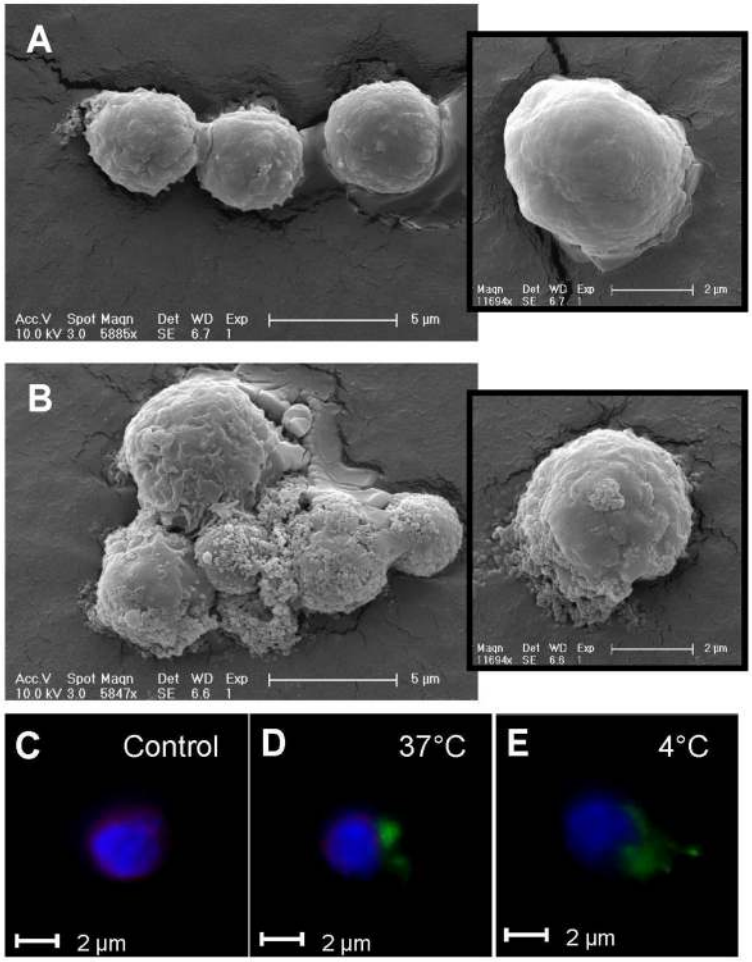

Figure 5. CD4-targeted NPs bind to CD4+ T cells

CD4+ T cells were imaged by SEM and fluorescent microscopy stimulation after incubation with or without CD4-targeted NPs. (A) Naïve CD4+ T cells were stimulated for 24 hours in the presence of antibodies only then fixed in 4% paraformaldehyde + 0.1% glutaraldehyde and imaged via SEM. (B) SEM of CD4+ T cells stimulated in the presence of CD4-targeted LIF-nano. For fluorescent experiments, CD4+ T cells were incubated alone (C) or with CD4-targeted nanoparticles encapsulating coumarin 6 (green) for 2 hours at either (D) 37°C or (E) 4°C. Cells were fixed with 4% paraformaldehyde and permeabilized using 0.1% Triton-X100. Cell nuclei and cytoskeleton were stained using DAPI (blue) and Texas-Red phalloidin (red), and cells were imaged at 40× magnification.

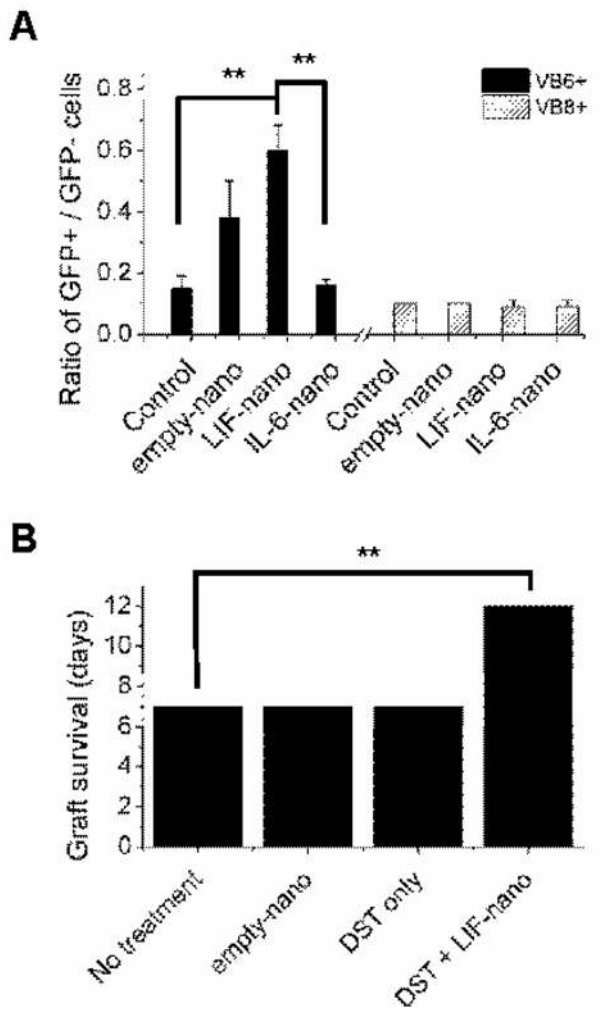

Figure 6. Localized delivery of LIF from CD4-targeted nanoparticles supports *in vivo* expansion of Foxp3+ T cells and supports allograft survival

(A) DBA/2 splenocytes were incubated for 15 minutes with CD4-targeted empty-nano, or LIF-nano, then infused (10^7 cells/mouse, i.v.) into BALB/c Foxp3-GFP mice (n=3 per group). Host lymph node cells were harvested 5 days later, and ratios of GFP+ vs. GFP- cells were calculated by FACS in the donor specific Vβ6 (black fill) or Vβ8 (striped fill) CD4+ T cell compartments (mean ± s.d.). Statistical significance was calculated by two-tailed t-test (** $p < 0.01$). (B) Vascularised heart grafts from BALB/c to CBA mice were rejected at 7d (no treatment controls; n=29: mean survival 6.86d). Animals received DST in similar fashion to the experiment in (A). A single i.v. dose of empty LIF-nano targeted to CD4 (empty nano; n=3: mean survival 7d) at time of grafting had no effect of graft survival. Donor-specific transfusion (DST only) alone had no effect as well (n=2: mean survival 7d). DST combined with LIF-nano therapy (DST + LIF-nano; n=3: mean survival 12.6d) resulted in significant prolongation of graft survival relative to the untreated control group ($p=<0.01$): analyses include Pearson Chi-Square $p<0.01$; and pExact statistics either one- or two-tailed $p<0.01$.

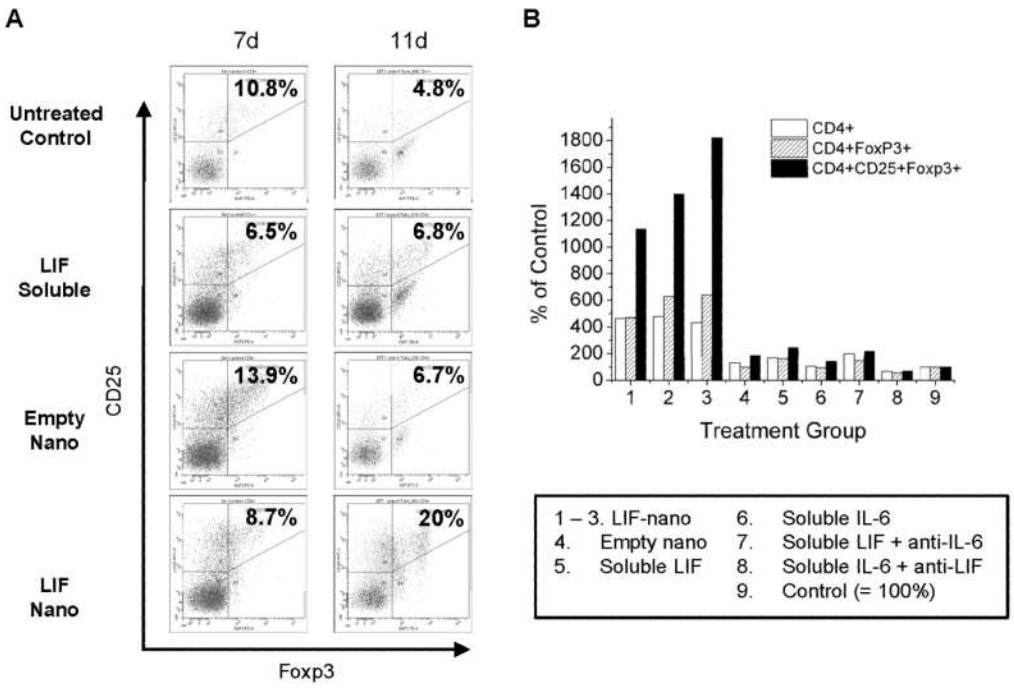

Figure 7. LIF-nano induce expansion of FOXP3+ CD4+ CD25+ T lymphocytes of the rhesus monkey

Peripheral blood lymphocytes (pbl) from 2 alloreactive rhesus monkeys were set up in a one way MLR (see methods). After 7d the cultures were boosted with irradiated donor pbl. Nine culture conditions were applied, as indicated. Both the LIF-nano and the empty-nano were targeted to CD4. The culture sets of 9 conditions were replicated for assaying by flow cytometry at 7d, prior to boosting (left-hand panels), and at 11d, 4d after boost (right-hand panels). (A) Analysis of the CD4+ cell population for FOXP3 (axis) and CD25 (abcissa) expression at 7d, and at 11d. (B) Total numbers of CD4+ cells in each culture at 11d shown as (i) all CD4+ cells (white fill); (ii) all dual CD4+ FOXP3+ cells (striped fill); and (iii) all triple positive CD4+ FOXP3+ CD25+ cells (black fill). Percentages are relative to controls.